Journal of Medicinal Chemistry

Article

Cite This: J. Med. Chem. XXXX, XXX, XXX−XXX

pubs.acs.org/jmc

Identification of 2-Imidazopyridine and 2-Aminopyridone Purinones as Potent Pan-Janus Kinase (JAK) Inhibitors for the Inhaled Treatment of Respiratory Diseases

Jordi Bach,[*,†] Paul Eastwood,[†] Jacob González,[†] Elena Gómez,[†] Juan Antonio Alonso,[†,#] Silvia Fonquerna,[†] Estrella Lozoya,[†] Adela Orellana,[†,▽] Mónica Maldonado,[†] Elena Calaf,[‡] Joan Albertí,[‡,○] Juan Pérez,[§] Ana Andrés,[∥,◆] Neus Prats,[∥,¶] Cristina Carreño,[⊥] Elena Calama,[⊥] Jorge De Alba,[⊥,⋈] Marta Calbet,[⊥] Montserrat Miralpeix,[⊥,⧓] and Isabel Ramis[⊥,⧖]

[†]Medicinal Chemistry & Screening, [‡]Pharmacokinetics & Metabolism, [§]Early Galenic Development, [∥]Pathology & Predictive Toxicology, and [⊥]Respiratory Therapeutic Group, Almirall R&D, Crta. Laureà Miró 408-410, Sant Feliu de Llobregat, 08980 Barcelona, Spain

Supporting Information

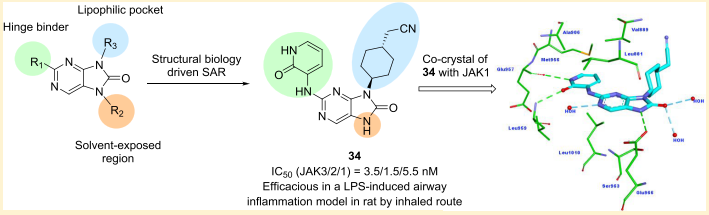

ABSTRACT: Janus kinases (JAKs) have a key role in regulating the expression and function of relevant inflammatory cytokines involved in asthma and chronic obstructive pulmonary disease. Herein are described the design, synthesis, and pharmacological evaluation of a series of novel purinone JAK inhibitors with profiles suitable for inhaled administration. Replacement of the imidazopyridine hinge binding motif present in the initial compounds of this series with a pyridone ring resulted in the mitigation of cell cytotoxicity. Further systematic structure−activity relationship (SAR) efforts driven by structural biology studies led to the discovery of pyridone **34**, a potent pan-JAK inhibitor with good selectivity, long lung retention time, low oral bioavailability, and proven efficacy in the lipopolysaccharide-induced rat model of airway inflammation by the inhaled route.

INTRODUCTION

Janus kinases (JAKs) are cytoplasmic protein tyrosine kinases associated with cytokine receptors. Following cytokine stimulation, JAKs phosphorylate signal transducers and activators of transcription (STAT), a family of transcription factors that dimerize, translocate to the nucleus, and activate gene transcription of inflammatory mediators. Four JAKs [namely, JAK1, 2, and 3, and tyrosine kinase 2 (Tyk2)] and seven STATs have been identified in the JAK−STAT pathway where different cytokine receptors are associated with specific combinations of paired JAKs (i.e., JAK1 and JAK3; JAK2 and JAK2) and STAT proteins.[1−7]

As JAKs are implicated in cell signaling processes that have a role in cancer as well as autoimmune and inflammatory diseases, enormous efforts have been devoted to the development of JAK inhibitors. As a consequence, several JAK inhibitors have progressed into clinical trials for the oral and topical treatment of myeloproliferative and autoimmune diseases and three of them, ruxolitinib (Incyte/Novartis), tofacitinib (Pfizer), and baricitinib (Incyte/Lilly), have reached the market for the oral treatment of myelofibrosis and rheumatoid arthritis.[8−10] On the other hand, the potential use of JAK inhibitors for the treatment of inflammatory respiratory diseases such as asthma and chronic obstructive pulmonary disease (COPD) has been far less explored. To the best of our knowledge, there are only three inhaled JAK inhibitors in preclinical studies: R256 from AstraZeneca/Rigel, a JAK1/3 inhibitor for moderate to severe asthma,[11,12] and two pan-JAK inhibitors from Pfizer (PF-06263276)[13] and Vectura (VR588)[14] for COPD and severe asthma, respectively.

Most of the proinflammatory cytokines that play a critical role as orchestrators of the persistent inflammation observed in asthma and COPD such as interleukins IL-2, IL-3, IL-4, IL-5, IL-6, IL-9, IL-12, IL-13, IL-22, and IL-23, granulocyte-macrophage colony-stimulating factor (GM-CSF), and interferon γ signal through JAKs (JAK1, 2, and 3).[15−17] Therefore, a pan-JAK inhibitor blocking multiple cytokine signaling has the potential to be a broad anti-inflammatory therapy for the treatment of these respiratory diseases. Substantial experimental evidence supports a role for JAK−STAT signaling in airway inflammation. In several animal models of allergic asthma and COPD, it has been shown that different JAK inhibitors are efficacious reducing the airway inflammation by

Received: March 27, 2019

DOI: 10.1021/acs.jmedchem.9b00533
J. Med. Chem. XXXX, XXX, XXX−XXX

Scheme 1. Novel Purinone JAK Inhibitor 2 Bearing an Imidazo[1,2-*a*]pyridine Ring as Hinge Binder Motif

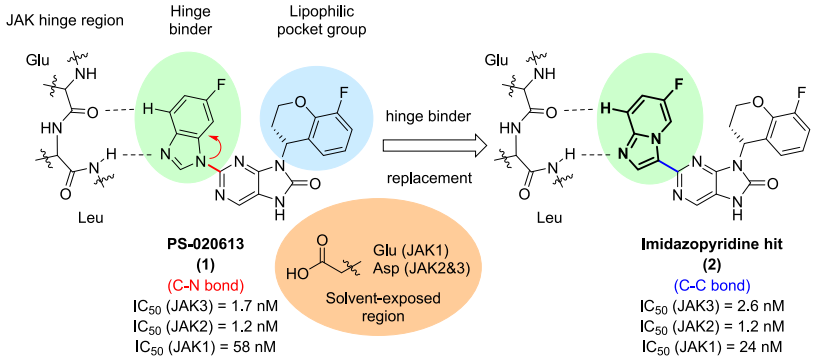

both the oral and inhaled routes.[11,12,14,18−21] Moreover, in human studies, it has been reported that overexpression of pSTAT3 in COPD lung tissue relates to the degree of airway inflammation and that total STAT-6 expression is increased in the bronchial epithelium of asthma patients compared to controls.[16,22−24]

Over the past few years, we have been interested in the development of inhaled pan-JAK inhibitors for the treatment of respiratory diseases with the main goal of developing a novel anti-inflammatory therapy with a favorable efficacy/safety ratio. Pan-JAK inhibition may have an additive effect on anti-inflammatory activity compared to JAK1/3 selective inhibitors as several relevant inflammatory mediators signal through JAK2 (i.e., IL-3, IL-5, and GM-CSF). On the other hand, systemic inhibition of JAK2 is associated with adverse effects such as thrombocytopenia, anemia, and hemoglobin reduction. In this sense, we selected the inhaled route of administration to avoid systemic exposure and limit the reported adverse effects observed in humans with oral JAK inhibitors.[25] Moreover, this strategy was supported by the fact that the majority of the target cells of JAK inhibitors are at the site of inflammation and that we and others have demonstrated that administration of JAK inhibitors by the inhaled route is also efficacious in animal models of asthma and COPD.[11,14,20] As a result, our efforts have been devoted to the search for pan-JAK inhibitors with a suitable profile for inhaled administration. It has been reported that physicochemical properties such as basicity, polarity, and/or aqueous solubility can be used to modulate retention times in the lung and assist in finding the right balance between lung and systemic exposure.[26] In this context, many inhaled drugs have a long duration period in the lung due to their low aqueous solubility, which causes inhaled particles to slowly dissolve and be absorbed into the lung tissue.

Following a low dissolution rate strategy for lung retention, in this paper, we describe the design, synthesis, and pharmacological evaluation of a series of novel purinone JAK inhibitors bearing an imidazopyridine or pyridone moiety as hinge binder. This work has resulted in the identification of pyridone **34**, a potent pan-JAK inhibitor with a long lung retention time, low oral bioavailability, and proven efficacy in the lipopolysaccharide (LPS)-induced rat model of airway inflammation by the inhaled route.

RESULTS AND DISCUSSION

The design of an imidazo[1,2-*a*]pyridine ring as hinge binder was inspired by PS-020613 (**1**), an early JAK3 inhibitor from Pharmacopeia (now Ligand Pharma) reported in the literature.[27] Docking studies with JAK3[28] suggested that the benzimidazole moiety would play a key role for the binding of **1** into the adenosine triphosphate (ATP) binding site of JAK enzymes. This structural motif would act as hinge binder through two interactions with two specific amino acids from the hinge region that are conserved among the different members of the JAK family: a classical hydrogen bond between the benzimidazole nitrogen and backbone NH of a leucine and a noncanonical interaction between a heteroaromatic hydrogen atom and the oxygen of the carbonyl group of a glutamic acid (Scheme 1). The presence of electron-withdrawing groups (i.e., a fluorine atom) attached to the benzimidazole core was contemplated as a way to improve the nonclassical interaction by increasing heteroaromatic H atom acidity. The chromane ring of **1** was postulated to fill a lipophilic pocket in the active site, whereas the purinone core would act as an optimal spacer keeping the appropriate distance between the hinge and lipophilic pocket moieties. The purinone ring might also have additional hydrophobic interactions with alkylic residues from amino acids located at the binding site. Nevertheless, the presence of the benzimidazole hinge binder was perceived as a concern for the chemical (and metabolic) stability of this compound as it could potentially act as leaving group via initial attack of a nucleophile on the purinone ring. Changing the hinge binder motif to an imidazo[1,2-*a*]pyridine ring as in compound **2** would prevent such potential instability.[29−31]

Initial hit **2** showed a similar profile of JAK inhibition to benzimidazole **1**, with potency against JAK2 and JAK3 in the low nanomolar range and somewhat less potent against JAK1 (IC_{50} = 24 nM), demonstrating that the proposed hinge binder replacement was well tolerated in terms of JAK activities. Unfortunately, compound **2** also proved to be cytotoxic in the cytotoxicity assay performed in Chinese hamster ovary (CHO) cells [IC_{50} (CHO) = 4 μM]. Based on these findings, two main goals were initially defined to improve the overall profile of **2**: (1) to increase JAK1 potency to identify truly pan-JAK inhibitors and (2) to reduce cytotoxicity to the desired level for a clinical candidate [IC_{50} (CHO) > 30 μM].

Expansion toward the solvent-exposed region was first explored to improve JAK1 potency by targeting new interactions with amino acids in this area. Docking studies performed with **2** led to the identification of glutamic acid 966 (Glu966) in JAK1 as an ideal target amino acid due to its proximity to the imidazolone ring and potential for forming ionic and hydrogen-bond interactions through the carboxylic acid side chain. As the equivalent amino acid in both JAK2 and JAK3 is aspartic acid (Asp939 and Asp912 respectively), this approach could also be employed to improve JAK2 and JAK3 potencies as well. Docking studies also suggested that Glu966

DOI: 10.1021/acs.jmedchem.9b00533
J. Med. Chem. XXXX, XXX, XXX−XXX

Table 1. Imidazopyridine Analogues: Solvent-Exposed Region SAR

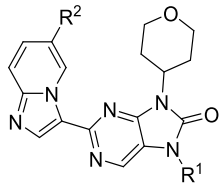

Compound	R^1	R^2	IC_{50} (JAK3) (nM)	IC_{50} (JAK2) (nM)	IC_{50} (JAK1) (nM)
3	H	CN	34	74	370
4	H	F	39	83	480
5	Me	CN	53	100	> 10 μM
6	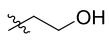	CN	59	77	850
7	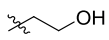	F	49	90	1700
8	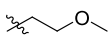	CN	47	190	> 10 μM
9	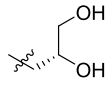	CN	80	81	1200
10	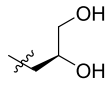	CN	96	75	2100
11	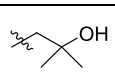	CN	80	380	5400
12	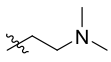	CN	490	800	> 10 μM
13	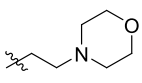	CN	260	340	> 10 μM

could be easily accessed through functionalization of the imidazolone NH, with a two-carbon chain as optimal spacer for the introduction of heteroatoms to reach the targeted interactions with the carboxylic acid. To test the hypothesis, a simple tetrahydropyran ring was used as a lipophilic pocket filling group and several functionalities with potential for forming hydrogen-bond interactions were introduced onto the imidazolone core, as shown in Table 1. In this initial structure–activity relationship (SAR) study, replacement of the fluorine atom of the hinge binder moiety by a more bulky electron-withdrawing cyano group was also evaluated.

Unsubstituted analogues **3** and **4** were first synthesized revealing that replacement of fluorine by a nitrile group had no impact on JAK inhibition as both molecules showed a similar profile of moderate JAK potencies. Interestingly, the introduction of a methyl group onto the imidazolone core (compound **5**) was well tolerated in terms of JAK2 and JAK3 potencies but resulted in a dramatic loss of JAK1 potency with respect to unsubstituted compound **3**. This loss of JAK1 potency was partially recovered while maintaining JAK2 and JAK3 potencies when a hydroxyethyl side chain was introduced (compounds **6** and **7**). JAK1 potency was lost again when **6** was converted into the corresponding methyl ether **8**, suggesting a role for the hydroxyl group in JAK1 inhibition. Further modifications of **6** such as introduction of an additional hydroxyl group (compounds **9** and **10**) or replacement of the primary alcohol by a tertiary alcohol (compound **11**) failed to improve JAK potencies. The scope of solvent-exposed groups was then expanded to basic side chains, but, unfortunately, tertiary amines **12** and **13** showed poor inhibitory potency against JAK2 and JAK3 and were inactive against JAK1. In summary, imidazolone functionalization to target new interactions with solvent-exposed amino acids (JAK1 Glu966, JAK2 Asp939, and JAK3 Asp912) failed to improve potency against JAK2 and JAK3 and was detrimental to JAK1 potency.

DOI: 10.1021/acs.jmedchem.9b00533
J. Med. Chem. XXXX, XXX, XXX−XXX

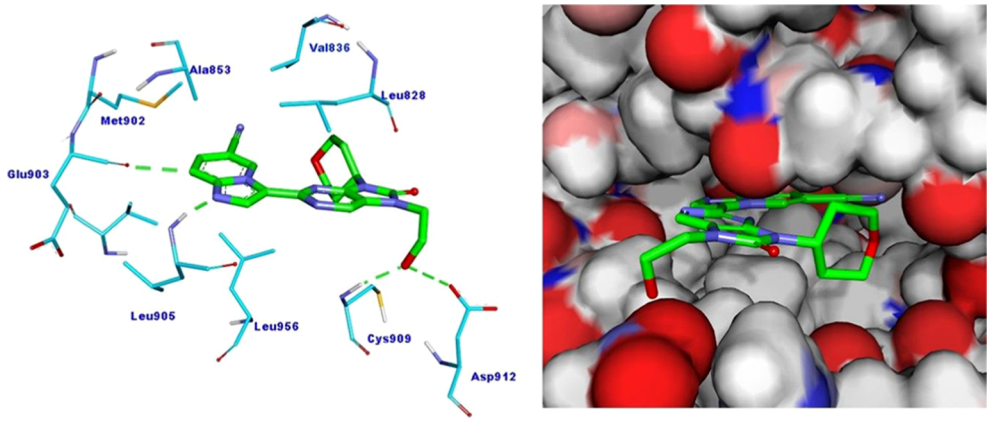

Figure 1. X-ray crystallographic structure of human JAK3 binding site in complex with **6** determined at 2.5 Å resolution [Protein Data Bank (PDB) entry 6HZV]. For clarity, only interacting amino acids are shown.

Inhibition of STAT-6 phosphorylation induced by IL-4 in human Ramos cells was used to assess JAK1/3 cellular potency of selected compounds from this series. Although both molecules were equipotent in JAK enzymatic assays, fluoro derivative **4** proved to be 3-fold more potent than the corresponding cyano analogue **3** (IC_{50} = 350 and 1100 nM, respectively) in this cellular assay.

To understand the results obtained, compound **6** was selected for structural biology studies. At this time point in the project, it was not feasible to obtain the X-ray crystallographic structure of human JAK1 with **6**, but we were successful in solving the co-crystal structure of this inhibitor with JAK3 at a resolution of 2.5 Å (Figure 1). The postulated binding mode was confirmed for this series of inhibitors with the tetrahydropyran ring occupying the lipophilic pocket and the imidazopyridine moiety acting as hinge binder through a classical hydrogen bond with backbone NH of Leu905 and a noncanonical interaction with the backbone carbonyl oxygen of Glu903. As expected, the purinone core acts as a spacer between the hinge and lipophilic pocket moieties and has no hydrogen-bond interactions with the enzyme. The co-crystal structure also confirmed the targeted interaction between the hydroxylated side chain of **6** and the carboxylic acid chain of solvent-exposed Asp912. Moreover, the hydroxyl group of **6** also showed an additional hydrogen-bond interaction with the backbone NH of cysteine 909. Despite these two additional interactions with solvent-exposed amino acids, no increase in JAK3 potency compared to unsubstituted compound **3** was seen. Regarding JAK1, it seems feasible that the targeted interaction with Glu966 could be achieved with molecules bearing a hydroxyl group (compounds **6**, **7**, and **9**−**11** in Table 1), but the dramatic loss of potency observed in molecules devoid of hydrogen-bond donors (compounds **5**, **8**, **12**, and **13**) could not be explained at this point.

A more successful approach to improve JAK1 potency was based on expanding the SAR in the lipophilic pocket (Table 2). For this SAR expansion exercise, 6-fluoroimidazopyridine was fixed as hinge binder due to the higher cellular potency observed for fluoro derivative **4** compared to cyano analogue **3**. Initial efforts were focused on modifying the tetrahydropyran ring of **4** to improve JAK activities. Although dimethyl substitution (compound **14**) and extrusion of the oxygen atom to give secondary and tertiary alcohols **15** and **16** improved on results obtained with **4**, the JAK potency profile of chromane **2** was not recovered. Taking into account that removal of the aromatic ring of **2** to yield **4** resulted in an important loss of JAK potencies and extrusion of the oxygen atom of the tetrahydropyran (THP) ring improved potency (compound **15**), alcohol **17** was designed and synthesized, and proved to be equipotent to **2**. Keeping in mind that the co-crystal structure of JAK3 with **6** unveiled that the tetrahydropyran oxygen is not involved in any key interactions with amino acids in the lipophilic pocket, a series of more flexible monocyclic compounds were explored (compounds **18**−**21**). Phenylethyl analogues **18** and **19** highlighted the importance of the absolute configuration of the chiral center on JAK potencies as **19**, having the same (R)-configuration as chromane **2**, proved to be at least 100-fold more potent against all JAKs than its enantiomer **18**. Results obtained with **19**, a molecule with a similar JAK inhibition profile to **2**, confirmed that the chromane oxygen is not essential for JAK potency. Encouraged by these results, an exhaustive SAR exploration of the aromatic ring was performed (data not shown) leading to the identification of pyridine **20** and pyrimidine **21** as both potent and balanced pan-JAK inhibitors. Both compounds fulfilled the defined goal in terms of JAK potencies, but cytotoxicity observed with these two molecules prevented them from further progression.

Since all potent analogues synthesized up to this point proved to be cytotoxic [IC_{50} (CHO) < 10 μM], further SAR expansion around the lipophilic pocket was not perceived as an approach that would solve this issue. Varying the hinge binder motif was thus explored as a possible way to mitigate cytotoxicity. In this context, cytotoxicity could be overcome without dramatically affecting JAK potencies when a more polar aminopyridone scaffold was introduced as a hinge binding group. This scaffold was conceptualized as a truncated analogue of the imidazopyridine ring that would keep key interactions with amino acids Leu and Glu in the hinge region through two classical hydrogen bonds, as shown in Scheme 2. The pyridone carbonyl group could act as hydrogen-bond acceptor with the backbone NH of leucine, whereas the pyridone NH could act as hydrogen-bond donor with the backbone carbonyl of the glutamic acid.

Analogues of potent imidazopyridine derivatives **2**, **17**, and **20** bearing an unsubstituted aminopyridone hinge binder were first synthesized (compounds **22**, **27**, and **28**) revealing a remarkable improvement in cytotoxicity for all cases, as shown in Table 3. Compared to the corresponding imidazopyridine analogues, chromane **22** proved to be equipotent, whereas a

DOI: 10.1021/acs.jmedchem.9b00533
J. Med. Chem. XXXX, XXX, XXX−XXX

Table 2. Imidazopyridine Analogues: Lipophilic Pocket SAR

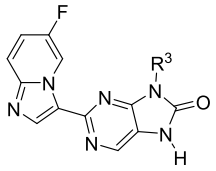

Ex	R^3	IC_{50} (JAK3) (nM)	IC_{50} (JAK2) (nM)	IC_{50} (JAK1) (nM)	Cytotoxicity CHO (μM)
2	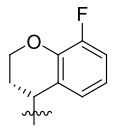	2.6	1.2	24	4.0
4		39	83	480	> 100
14	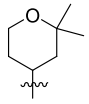	4.9	4.8	74	17
15	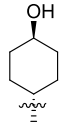	8.4	5.4	150	100
16	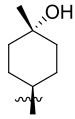	64	13	79	16
17	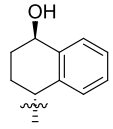	1.0	0.8	18	8.0
18	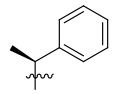	420	68	> 10000	23
19	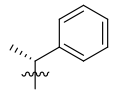	2.7	0.7	54	7.7
20	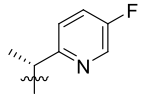	3.0	0.3	5.5	7.7
21	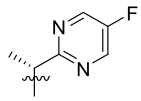	3.9	0.6	3.5	4.3

decrease in JAK potencies was observed for the other two molecules: moderate for alcohol **27**, more pronounced for fluoropyridine **28**. The impact of pyridone substitution on JAK potencies was then evaluated. Based on docking studies, introduction of small groups at the 5-position of the pyridone ring was explored. Regarding chromane derivatives, an improvement in JAK enzymatic and cellular potencies while keeping cytotoxicity at the desired level was achieved with the incorporation of electron-withdrawing groups such as halogen atoms (compounds **23** and **24**) at this position. On the other hand, an important decrease of JAK1 potency was observed for the methyl and methoxy derivatives **25** and **26**. A similar effect on JAK potencies was observed when halogen atoms were introduced at the pyridone hinge binder of molecules bearing the chiral fluoropyridine instead of the chromane ring (compounds **29** and **30**). For both lipophilic pocket groups, the presence of a chlorine atom in the 5-position of the pyridone ring provided the best results in terms of cellular potency in the JAK1/3 IL-4/STAT-6 Ramos assay. At this point, SAR studies varying the lipophilic pocket moiety were expanded taking advantage of reported co-crystal structures of tofacitinib with the four members of the JAK family.[32,33] In this sense, compounds **31** and **34** were designed to position a cyano group toward the glycine-rich loop region, mimicking tofacitinib's cyanoacetamide (Figure 2). Although both molecules proved to be potent and noncytotoxic pan-JAK inhibitors, they exhibited a different behavior when tested in the cellular assay. While cyclohexane derivative **34** was the most potent compound identified in this series, chiral piperidine **31** suffered from poor cellular potency. Dramatic differences in permeability observed for these two compounds in the parallel artificial membrane permeability (PAMPA) assay (P_{app} = 0.03 × 10^{-6} cm/s for **31**; 0.61 × 10^{-6} cm/s for **34**) likely account for the difference seen in the cellular assay. The corresponding enantiomer of **31** was synthesized (compound **33**), which resulted in a drop of potency in all JAKs. With the aim of increasing cellular potency, a chlorine atom was now introduced onto the pyridone ring of **31** and **34**. Unfortunately, chlorinated compounds **32** and **35** failed to improve the overall profile of JAK enzymatic and cellular potencies compared to the corresponding unsubstituted analogues.

Among the most potent pyridones identified, compound **34** was selected for structural biology studies with JAK1. Compound **34** was successfully co-crystallized with human JAK1 at a 2.5 Å resolution (Figure 3), and the relevant structural information obtained from these studies provided a better understanding of JAK1 SAR. The expected binding mode for this family of inhibitors was confirmed with the pyridone ring acting as a hinge binding motif through two classical hydrogen-bond interactions with the backbone carbonyl group of Glu957 and the backbone NH of Leu959. Interestingly, the co-crystal structure unveiled an unexpected hydrogen-bonding interaction between the imidazolone NH and the carboxylic acid side chain of solvent-exposed Glu966, the amino acid that was selected as a target for possible interactions in early SAR studies (vide supra). This additional interaction would be lost in molecules where the imidazolone ring is substituted (e.g., methyl derivative **5**), resulting in the observed loss of JAK1 potency, which can be partially recovered in compounds that bear a hydrogen-bond donor as part of the solvent-exposed group. As expected, the cyano group present in **34** does not have any additional hydrogen-bond interaction but is filling a cavity in the lipophilic pocket region, in proximity to the glycine loop.

Due to a balanced profile of JAK enzymatic potencies and remarkable cellular potency in the JAK1/3 assay, compound

DOI: 10.1021/acs.jmedchem.9b00533
J. Med. Chem. XXXX, XXX, XXX−XXX

Scheme 2. Novel Purinone JAK Inhibitors Bearing an Aminopyridone Ring as Hinge Binder

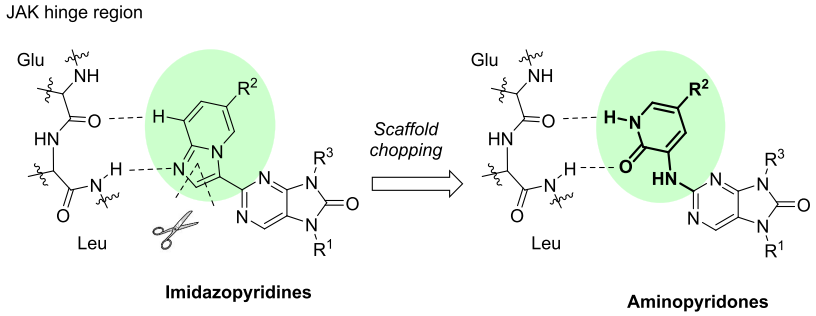

34 was selected for further profiling. Regarding additional enzymatic assays, **34** was found to be less potent against Tyk2 (IC_{50} = 130 nM) and showed promising selectivity in a panel of 36 human kinases, which included targets commonly inhibited by JAK inhibitors (Figure 4).[34] In this study, performed at Millipore, only Aurora-A, FGFR1, Flt4, Ret, and TrkA were inhibited >75% at a compound concentration of 10 μM and were identified as potential off-target activities.

JAK2/2 cellular activity of **34** was assessed by measuring the inhibition of phosphorylation of STAT-5 in monocytes isolated from human peripheral blood mononuclear cells stimulated with GM-CSF and resulted in a 5-fold drop of potency compared to JAK1/3 cellular activity (IC_{50} = 219 nM). In the search for nonkinase off-target activities, compound **34** showed weak activity against potassium (hERG), sodium ($Nav_{1.5}$), and calcium ($Cav_{1.2}$) ion channels (less than 15% inhibition when tested at a 10 μM concentration), indicating a low potential to cause cardiovascular side effects. In addition, **34** also proved to be clean when tested at a 10 μM concentration against a panel of 55 diverse G protein-coupled receptors, transporters, and ion channels (Cerep ExpresSProfile). Furthermore, **34** was not genotoxic in exploratory Ames and GreenScreen HC testing.[35]

In terms of physicochemical properties, compound **34** has moderate lipophilicity (Log $D_{7.4}$ = 2.1) and excellent chemical stability at all pHs tested (pH = 1.2, 5.5, 7.4, and 9.0). Despite its poor solubility at physiological pH (pH=7.4; 0 mg/mL), **34** showed sufficient solubility in various formulations used for in vivo testing and its high melting point (319−332 °C) allows this molecule to be micronized for potential use in a dry powder inhaler.

The absorption, distribution, metabolism, and excretion properties of **34** were also investigated and are summarized in Table 4. In vitro, **34** showed moderate permeability in the PAMPA assay (P_{app} = 0.61 × 10^{-6} cm/s), moderate plasma protein binding (PPB, 79% in rat; 83% in human), and low metabolism in liver microsomes (17% rat; 21% human). To evaluate the suitability of **34** for inhaled delivery in the in vivo animal model, both oral and intratracheal (it) pharmacokinetic (PK) studies were performed in rat. Interestingly, a low oral bioavailability was observed for **34** as very low levels of compound were found in plasma after per os (po) administration of a 30 mg/kg dose (AUC_{inf} = 32 ng h/mL; C_{max} = 7 ng/mL). Moreover, **34** was well retained in the lung when administered intratracheally as a nanosuspension at a 0.41 mg/kg dose ($t_{1/2}$ = 16.3 h) and showed an excellent lung/plasma partition (11 364) ideal for inhaled administration (Figure 5).

Due to a favorable pharmacokinetic profile for inhaled administration, compound **34** was further progressed to an acute model of inhaled lipopolysaccharide (LPS)-induced airway inflammation in rats. In this model, rats were exposed to an aerosol of LPS that induces an increase of neutrophils in bronchoalveolar lavage fluid (BALF) that peaks after 4 h of LPS challenge. Further study of BALF shows an increase of several cytokines that signal through the JAK−STAT pathway, such as IL-6.[21] Compound **34** was administered intratracheally as an aerosolized nanosuspension, using phosphate-buffered saline containing 0.2% Tween 80 and 0.3% methylcellulose as vehicle, at doses of 0.01, 0.1, 1, and 3 mg/kg 1 h before rats were exposed to the LPS challenge. Neutrophils were counted and IL-6 levels were measured in BALF samples collected 4 h after LPS exposure. Two additional groups of rats were also challenged with aerosolized LPS: one was administered only with vehicle to determine the maximum effect of LPS challenge on neutrophil count, whereas the other was dosed intratracheally with fluticasone (0.1 mg/kg) and used as positive control. Compound **34** exhibited a dose-dependent inhibition of LPS-induced neutrophilia with a maximum effect at the 3 mg/kg dose (56% inhibition, Figure 6). At the same dose, a significant reduction of IL-6 levels in BALF (62%) was observed. Intratracheal pharmacokinetic studies performed with **34** at the efficacious dose of 3 mg/kg confirmed the high lung/plasma partition observed in previous studies (AUC_{lung}: 14 557 μg h/g, AUC_{plasma}: 406 ng h/mL, AUC_{lung}/AUC_{plasma}: 35 856), with lung levels of compound well above and unbound plasma levels [C_{max} (plasma): 57 ng/mL] below the cellular IC_{50} up to 24 h post administration, suggesting that the observed efficacy is due to a local inhibition of JAK kinases in the lung. The results obtained with **34** in the LPS-induced airway inflammation model support the potential use of inhaled JAK inhibitors for the treatment of respiratory inflammatory diseases.

CHEMISTRY

Initial imidazopyridine compounds **2**−**4** were synthesized as shown in Scheme 3. A regioselective nucleophilic aromatic substitution (S_NAr) reaction between the corresponding amines and activated dichloropyrimidine **36** furnished compounds **37** and **38**. Catalytic hydrogenation of the nitro group in the presence of zinc(II) bromide led to dianilines **39** and **40**, which were treated with carbonyldiimidazole (CDI) to form purinone intermediates **41** and **42**, respectively. After 2-(trimethylsilyl)ethoxymethyl (SEM) protection of the imidazolone NH, hinge binder motifs were introduced in one step from commercial imidazopyridines **45** and **46** through a palladium-catalyzed heteroaryl Heck reaction using tetrakis-

DOI: 10.1021/acs.jmedchem.9b00533
J. Med. Chem. XXXX, XXX, XXX−XXX

Table 3. Aminopyridones: Hinge Binder and Lipophilic Pocket SAR

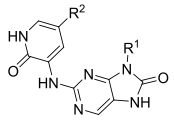

Ex	R^1	R^2	IC_{50} (JAK3) (nM)	IC_{50} (JAK2) (nM)	IC_{50} (JAK1) (nM)	IC_{50} IL-4 / Ramos (nM)	IC_{50} Cytotoxicity CHO (μM)
22		H	2.8	3.2	28	96	> 100
23		F	1.1	2.3	8.7	76	> 100
24		Cl	1.1	1.3	54	44	36
25		Me	2.4	1.9	180	130	51
26		OMe	16	24	750	ND	ND
27		H	3.4	4.3	49	130	> 100
28	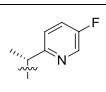	H	40	5.3	41	140	> 100
29	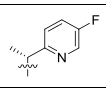	F	6.0	4.8	31	130	> 100
30	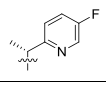	Cl	1.4	2.0	12	68	33
31		H	3.6	1.7	9.4	760	> 100
32	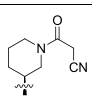	Cl	1.4	2.4	20	3400	> 100
33		H	18	7.4	39	3400	ND
34	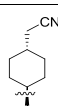	H	3.5	1.5	5.5	41	> 100
35	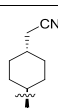	Cl	0.7	3.6	25	46	> 100

(triphenylphosphine)palladium(0) as catalyst and potassium acetate as base at 150 °C. Finally, SEM removal using tetra-*n*-butylammonium fluoride (TBAF) or under aqueous acidic conditions afforded compounds **2**–**4**.

Compounds synthesized to target new interactions in the solvent-exposed region were prepared from common intermediate **42**, as described in Scheme 4. Compounds **5** and **11**–**13** were obtained through alkylation of the imidazolone NH of **42** with the corresponding halo derivatives followed by a heteroaryl Heck reaction to introduce the cyanoimidazopyridine hinge binder moiety. The same sequence was used to synthesize alcohols **6** and **7** and diols **9** and **10**. For these molecules, a final deprotection step under acidic conditions was needed as both the alcohol and diol functionalities were introduced protected as tetrahydropyranyl ethers and isopropylidene acetals, respectively. In the particular case of compound **8**, this molecule was synthesized in one step by alkylation of **3** with 1-bromo-2-methoxyethane.

Imidazopyridines synthesized to explore lipophilic pocket SAR were prepared following an alternative synthetic approach based on intermediate **63** (Scheme 5). This approach would allow variation of groups that would ultimately reside in the lipophilic pocket at the last steps of the synthesis. Treatment of aminopyridine **57** with 3-methoxyacrylonitrile **58** in the presence of *N*-bromosuccinimide (NBS) furnished cyanoimidazopyridine **59**, which was converted into amidine **60** by reaction with catalytic sodium methoxide in methanol followed by addition of ammonium chloride. Cyclization of **60** with nitroacrylate **61** provided pyridone **62**, which was transformed into chloropyrimidine **63** by treatment with phosphorus oxychloride.

To explore SAR in the lipophilic pocket, a diverse set of groups were introduced by S_NAr reaction of the corresponding amines with **63**, as shown in Scheme 6. Nitro reduction with tin(II) chloride in ethanol or by catalytic hydrogenation followed by cyclization with carbonyldiimidazole yielded compounds **14**, **16**, and **18**–**21**.

Following the same synthetic approach, *tert*-butyldiphenylsilyl (TBDPS)-protected amino alcohols **76** and **80** were used for the synthesis of compounds **15** and **17** (Scheme 7). After nitro reduction and carbonyldiimidazole cyclization, the TBDPS-protecting group was removed by treatment with TBAF or cesium fluoride to yield alcohols **15** and **17**, respectively.

The majority of purinones bearing an aminopyridone hinge binder motif were prepared as described in Scheme 8. S_NAr reaction of the corresponding amines with activated pyrimidine **36** furnished **37** and **84**–**85**. Elaboration of these intermediates to the corresponding SEM-protected purinones **43** and **90**–**91** proceeded using the same methods as described above (Scheme 3). In the key step of these syntheses, a palladium-catalyzed Buchwald–Hartwig amination reaction of anilines **92**–**96** with the SEM-protected chloropurinones yielded advanced intermediates **97**–**105**. Finally, SEM deprotection of these molecules by treatment with either TBAF or trifluoroacetic acid followed by deprotection of the methoxy groups by reaction with trimethylsilyl chloride (TMSCl) and sodium iodide at 80 °C provided compounds **22**–**26**, **28**–**30**, and **35**.

The synthesis of aminopyridines **93**–**96**, which are key intermediates utilized in the synthesis of pyridones **22**–**35** along with commercially available 2-methoxy-3-aminopyridine **92**, is outlined in Scheme 9. The reaction of chloropyridines **115** and **116** with sodium methoxide followed by reduction of the nitro group via catalytic hydrogenation afforded aminopyridines **94** and **95**, where the R group is a chloro atom and a methyl group, respectively. Oxidation of commercially

DOI: 10.1021/acs.jmedchem.9b00533
J. Med. Chem. XXXX, XXX, XXX–XXX

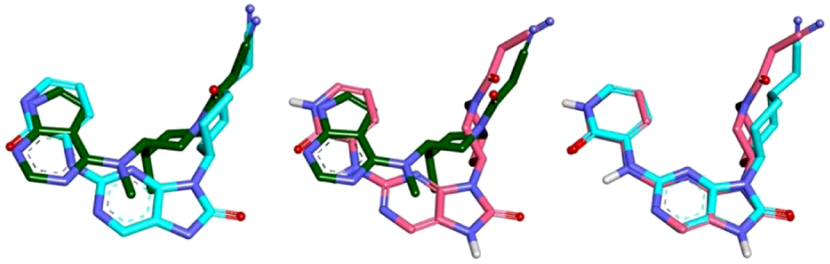

Figure 2. Overlapping studies with compounds **31** (pink), **34** (blue), and tofacitinib (green) showing similar arrangement of nitrile group in all of the cases and also carbonyl disposition of amides in **31** and tofacitinib.

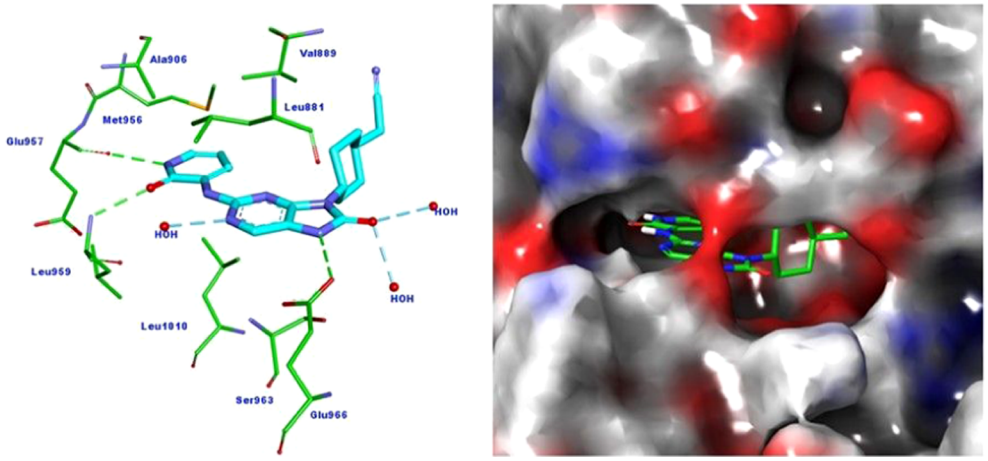

Figure 3. X-ray crystallographic structure of human JAK1 binding site complexed with compound **34** determined at 2.2 Å resolution (PDB entry 6HZU). For clarity, only interacting amino acids are shown.

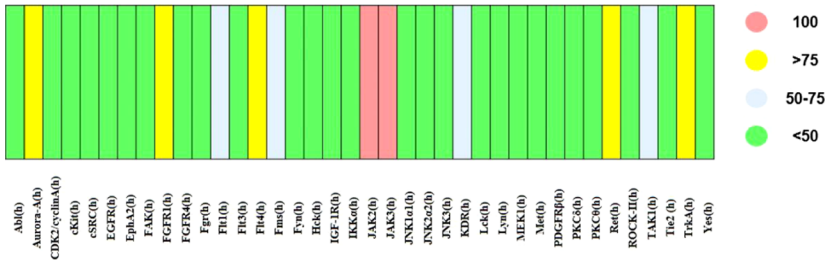

Figure 4. Heat map showing the kinase inhibition profile of **34** dosed at 10 μM against a panel of 38 kinases at [ATP] = K_m. Colors correspond to % inhibition of a given kinase as shown in the legend.

Table 4. In Vitro and in Vivo Profiles of Compound 34

	in vitro			in vivo	
assay	PAMPA	% PPB	% metabolism (LM)	po PK (rat), 30 mg/kg	it PK (rat), 0.41 mg/kg nanosuspension
value	P_{app} = 0.61 × 10^{-6} cm/s	79 (R) 83 (H)	17 (R) 21 (H)	AUC_{inf} = 32 ng h/mL C_{max} = 7 ng/mL	$t_{1/2}$ = 16.3 h; AUC_{lung} = 1341 μg h/g AUC_{plasma} = 118 ng h/mL; AUC_{lung}/AUC_{plasma} = 11 364

available boronate **117** with hydrogen peroxide resulted in hydroxypyridine **118**, which was alkylated with methyl iodide to yield dimethoxypyridine **124**. Reduction of the nitro group of **124** by catalytic hydrogenation as described above provided aminopyridine **96**. For the particular case where R is a fluorine atom, nitration of hydroxypyridine **119** yielded nitro intermediate **120**. Selective O-alkylation of **120** was achieved using methyl iodide as alkylating agent and silver carbonate as base at room temperature to give **121**, which was converted to aminopyridine **93** as described above.

Aminonitrile **129**, a key intermediate for the synthesis of compounds **34** and **35**, was synthesized in four steps starting from commercial amino alcohol **125** (Scheme 10). The amino group of **125** was selectively protected by reaction with 1 equiv of di-*tert*-butyl dicarbonate, and the resultant alcohol **126** was converted into tosylate **127** by reaction with *p*-toluenesulfonyl chloride. The reaction of **127** with sodium cyanide followed by removal of the *tert*-butyloxycarbonyl (Boc) group under acidic conditions afforded aminonitrile **129**.

Aminopyridones **31**−**34** were prepared following an alternative synthetic approach in which the lipophilic pocket group was introduced after the hinge binder moiety, as illustrated in Scheme 11. In this approach, pyrimidine **36** was first converted into thiocyanate **130** to reverse pyrimidine

DOI: 10.1021/acs.jmedchem.9b00533
J. Med. Chem. XXXX, XXX, XXX−XXX

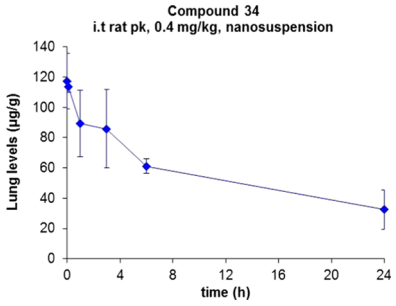

Figure 5. Pharmacokinetic profile of **34** after intratracheal administration as a nanosuspension.

reactivity and direct hinge binder introduction to the 2-position. S_NAr reaction of aminopyridines **92** and **94** with pyrimidine **130** at 0 °C proceeded with moderate yields but excellent regioselectivity to the desired thiocyanates **131** and **132**. The reaction of these thiocyanates with the corresponding amines yielded intermediates **133**−**136**. Nitro reduction by catalytic hydrogenation followed by cyclization with carbonyldiimidazole afforded purinones **141**−**144**, in which both the hinge binder and the lipophilic moieties have been introduced by S_NAr reactions. For purinones **141**−**143**, where the purinone N-substituent is Boc-protected piperidine, a one-pot, double deprotection was performed under acidic conditions to give piperidines **145**−**147**, which were further converted into cyanoacetamides **31**−**33** by reaction with 2,5-dioxopyrrolidin-1-yl 2-cyanoacetamide. For the particular case of purinone **144**, with a cyclohexylacetonitrile N-substituent, methoxy deprotection under standard conditions provided compound **34**.

Synthesis of compound **27** is outlined in Scheme 12. The reaction of pyrimidine **36** with amine **80** provided the desired regioisomer **148**, which was elaborated as detailed above to provide compound **153**. The SEM and TBDPS groups were simultaneously removed by treatment of **153** with TBAF in tetrahydrofuran, and subsequent deprotection of the benzyl group by catalytic hydrogenation yielded the desired alcohol **27**.

CONCLUSIONS

Herein are described the discovery and progression of a series of novel purinone pan-JAK inhibitors with the potential for treatment of respiratory diseases by the inhaled route. Replacement of the benzimidazole in Pharmacopeia's JAK3 inhibitor PS-020613 by an imidazo[1,2-*a*]pyridine ring was designed as a way to improve potential instability issues. This bioisosteric hinge binder replacement was well tolerated in terms of JAK potencies giving rise to **2**, a compound with potencies against JAK2 and JAK3 in the low nanomolar range but 20-fold less potent against JAK1. In our search for a potent pan-JAK inhibitor, systematic SAR efforts driven by structural biology studies were performed to improve the JAK1 potency of **2**. Initial studies which attempted to target new interactions with the solvent-exposed amino acid Glu966 in JAK1 were unsuccessful. On the other hand, compounds with adequate JAK potencies were identified by varying the groups in the lipophilic pocket, but unfortunately, the cytotoxicity observed with these molecules prevented them for further progression. This cytotoxicity could be overcome without dramatically affecting JAK potencies by the introduction of an aminopyridone ring as the hinge binding motif. Further, SAR expansion in the lipophilic pocket region led to the discovery of pyridone **34**, a potent pan-JAK inhibitor with good selectivity, long lung retention time, low systemic exposure, and proven efficacy in the LPS model of airway inflammation by the intratracheal route. Furthermore, **34** was successfully co-crystallized with JAK1, confirming the expected binding mode for this series of inhibitors and providing a better understanding of JAK1 SAR. Pyridone **34** underwent further characterization to assess the potential as a preclinical development candidate.

EXPERIMENTAL SECTION

General Experimental. The care of animals was undertaken in compliance with the European Committee Directive 2010/63/EU and the Spanish and autonomous Catalan laws (Real Decreto 53/2013 and Decret 214/1997). Experimental procedures were reviewed by the Animal Welfare Body of Almirall and approved by the competent authority.

All test compounds have purity >95%. The purity of compounds was determined by high-performance liquid chromatography (HPLC) or ultraperformance liquid chromatography (UPLC) analysis. HPLC analyses were performed using a Waters 2795 system equipped with a Symmetry C-18 (2.1 × 100 mm, 3.5 µM) column. The mobile phases were (B): formic acid (0.4 mL), ammonia (0.1 mL), methanol (500 mL), and acetonitrile (500 mL) and (A): formic acid (0.5 mL), ammonia (0.125 mL), and water (1000 mL). A gradient between 0 and 95% of B was used. The flow rate was 0.4 mL/min. The run time was 30 min. The injection volume was 5 µL. A Waters 2996 diode array was used as a UV detector. Chromatograms were processed at 210 nm. Mass spectra of the chromatograms were acquired using positive and negative electrospray ionization (ESI) in a Waters ZQ detector coupled to the HPLC. UPLC analyses were performed using a Waters Acquity UPLC system coupled to an SQD mass spectrometer detector. The system was equipped with an ACQUITY UPLC BEH C-18 (2.1 × 50 mm, 1.7 mm) column. The mobile

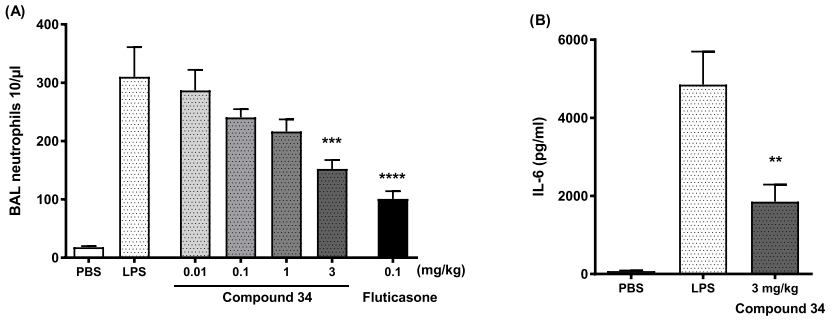

Figure 6. Effects of intratracheal administration of compound **34** on (A) neutrophil count in BALF; n = 14−16/group and (B) IL-6 levels in BALF; n = 9−12/group, in the rat LPS challenge model. *** $P < 0.001$, ** $P < 0.01$ treated vs LPS group, analysis of variance + Dunnett's test.

DOI: 10.1021/acs.jmedchem.9b00533
J. Med. Chem. XXXX, XXX, XXX−XXX

Scheme 3. Synthesis of Initial Imidazopyridine Compounds 2−4[a]

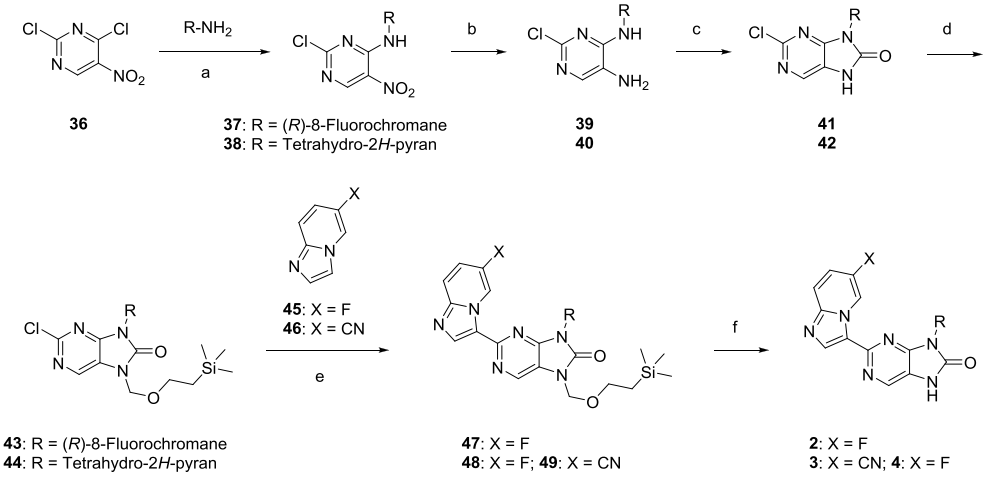

[a]Reagents and conditions: (a) R−NH_2, *N*,*N*-diisopropylethylamine (DIEA), CH_2Cl_2, −78 °C to room temperature (rt), 91−95%; (b) H_2, Pd/C, $ZnBr_2$, EtOAc, rt, 97−99%; (c) CDI, THF or CH_3CN, 80 °C, 65−80%; (d) NaH, SEM−Cl, dimethylformamide (DMF), 0 °C to rt, 86−90%; (e) $Pd(PPh_3)_4$, KOAc, dimethylacetamide (DMA), 150 °C, 35−68%; (f) TBAF, CH_2Cl_2, rt to 70 °C or HCl 4 N, 70 °C, 32−83%.

Scheme 4. Imidazopyridines: Synthesis of N-Alkylated Purinones[a]

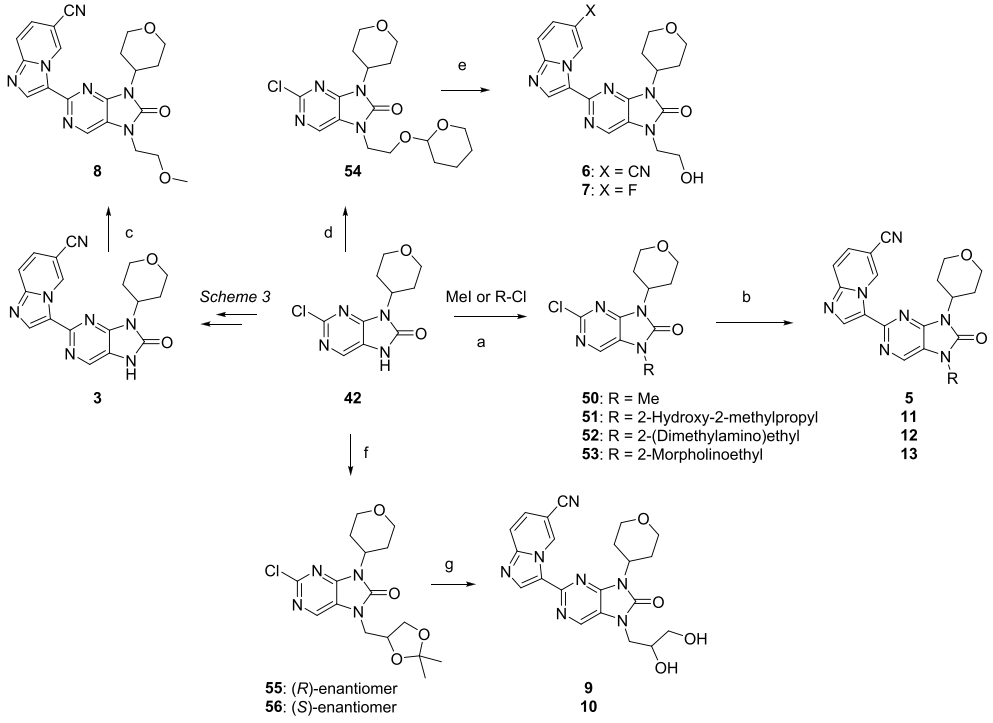

[a]Reagents and conditions: (a) MeI, NaH, DMF, 0 °C or R−Cl, K_2CO_3, DMF, rt to 90 °C, 45−88%; (b) **46**, $Pd(PPh_3)_4$, KOAc, DMA, 150 °C, 11−40%; (c) 1-bromo-2-methoxyethane, K_2CO_3, DMF, rt, 60%; (d) 2-(2-bromoethoxy)tetrahydro-2*H*-pyran, K_2CO_3, DMF, 90 °C, 90%; (e) **45** or **46**, $Pd(PPh_3)_4$, KOAc, DMA, 150 °C then 2 N HCl, rt, 14−77%; (f) (*R*)- or (*S*)-4-(chloromethyl)-2,2-dimethyl-1,3-dioxolane, K_2CO_3, DMF, 90 °C, 52−67%; (g) **46**, $Pd(PPh_3)_4$, KOAc, DMA, 150 °C then 4 N HCl, rt to 70 °C, 43−47%.

phases were (B): formic acid (0.4 mL), ammonia (0.1 mL), methanol (500 mL), and acetonitrile (500 mL) and (A): formic acid (0.5 mL), ammonia (0.125 mL), and water (1000 mL). A gradient between 5 and 95% of B was used. The flow rate was 0.65 mL/min. The run time was 5 min. The injection volume was 0.5 μL. Chromatograms were processed at 210 nm. Mass spectra of the chromatograms were acquired using positive and negative electrospray ionization. Reaction products were purified, when necessary, by flash chromatography on silica gel (40−63 μm) with the solvent system indicated. Purifications in reverse phase were made in a Biotage SP1 automated purification system equipped with a C-18 column and using a standard gradient of water−acetonitrile/MeOH (1:1) (0.1% v/v ammonium formate both phases) from 0 to 100% acetonitrile/MeOH (1:1) in 80 column volumes. Other conditions are stated explicitly in the text. Preparative HPLC−mass spectrometry (MS) was performed on a Waters instrument equipped with a 2767 injector/collector, a 2525 binary gradient pump, a 2996 PDA detector, a 515 pump as a make-up pump, and a ZQ4000 mass spectrometer detector. ^1H nuclear magnetic resonance (NMR) spectra were recorded on a Gemini 200 MHz, Gemini-2000 300 MHz, Varian Mercury plus 400 MHz, or an Agilent VNMRS-DD2 600 MHz spectrometer. Tetramethylsilane was used as reference. Chemical shifts δ are in parts per million (ppm);

DOI: 10.1021/acs.jmedchem.9b00533
J. Med. Chem. XXXX, XXX, XXX−XXX

Scheme 5. Imidazopyridines: Synthesis of Common Intermediate 63[a]

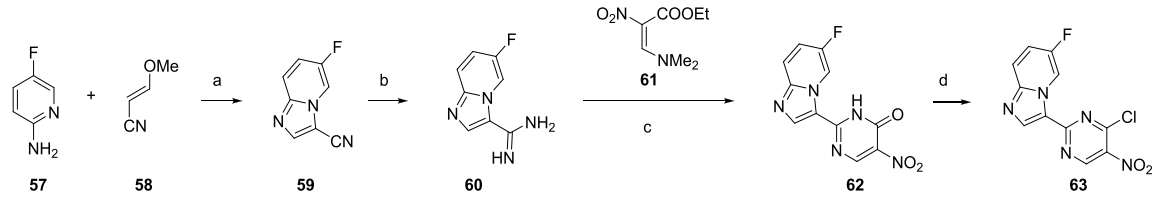

[a]Reagents and conditions: (a) NBS, dioxane, H_2O, 0−60 °C, 79%; (b) NaOMe, NH_4Cl, MeOH, reflux, 90%; (c) Et_3N, EtOH, 90 °C, 60%; (d) $POCl_3$, 90 °C, 57%.

Scheme 6. Imidazopyridines: Synthesis of 9-Substituted Purinones[a]

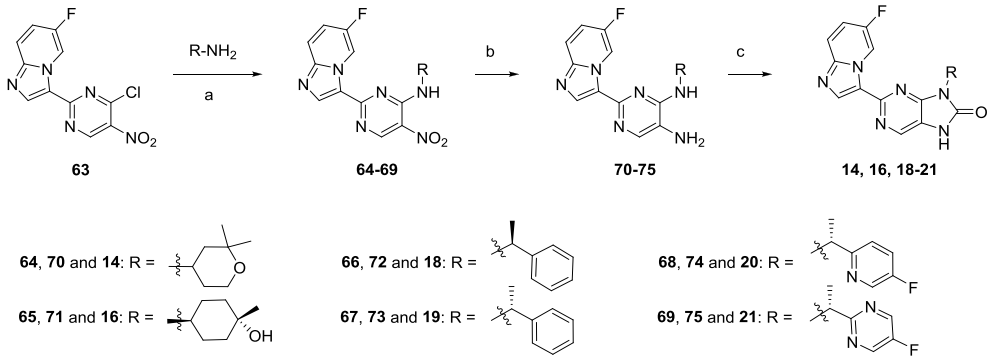

[a]Reagents and conditions: (a) R−NH_2, DIEA, THF, rt, 72−93%; (b) $SnCl_2$, EtOH, 80 °C or H_2, Pd/C, EtOH, 51−97%; (c) CDI, CH_3CN, 80 °C, 30−74%.

Scheme 7. Imidazopyridines: Synthesis of Alcohols 15 and 17[a]

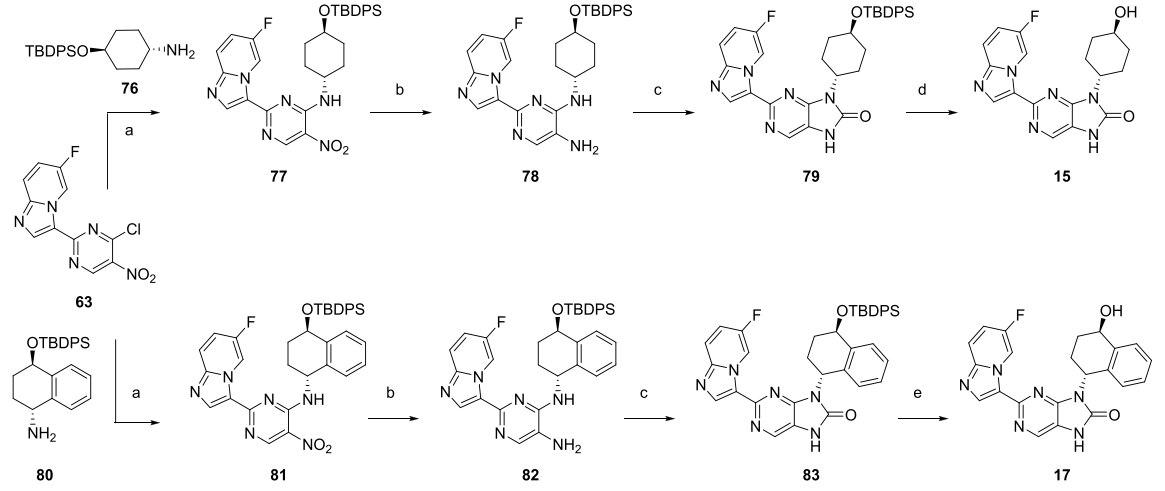

[a]Reagents and conditions: (a) DIEA, THF, rt, 81−87%; (b) H_2, Pd/C, EtOH, 75−82%; (c) CDI, CH_3CN, 80 °C, 67−91%; (d) TBAF, THF, rt, 55%; (e) CsF, DMF, 60 °C, 47%.

the following abbreviations are used: singlet (s), doublet (d), triplet (t), quartet (q), double doublet (dd), quintet (quin), multiplet (m), broad signal (br s), apparent signal (app). ^{13}C Nuclear magnetic resonance spectra were recorded on an Agilent VNMRS-DD2 600 MHz spectrometer equipped with a cold probe. Spectra were referenced to the DMSO residual signal at δ = 39.9 ppm. Mass spectra (m/z) were recorded on Micromass ZMD or Waters ZQ mass spectrometer using ESI ionization. Isotopic distributions are quoted for the mass ion of the lowest-molecular-weight isotope (^{35}Cl and ^{79}Br) and the number of isotopes detected. High-resolution mass spectra (HRMS) were obtained from 1 μL of a 0.05 mg/mL methanolic solution of each analyzed compound injected in a UHPLC 1290 Infinity (Agilent Technologies) coupled to a 6220 Accurate-Mass time-of-flight (TOF) mass spectrometer (Agilent Technologies). A dual ESI in positive mode was used as ionization source. TOF acquisition conditions were: scan acquisition mode (70−3000 Da, scan rate: 1.00 spec/s), gas temp: 300 °C, gas flow: 8 L/min, nebulizer: 40 psi, V cap: 2000 V, fragmentor: 150 V, skimmer 1: 65 V, octopole radio frequency peak: 250 V, and reference masses: m/z 121.050873 and 922.009798.

Chemistry: Synthetic Procedures to 34. Additional experimental procedures for all novel compounds prepared during the course of this work can be found in the Supporting Information.

*tert-Butyl (1r,4r)-4-(Hydroxymethyl)cyclohexylcarbamate (**126**).* Di-*tert*-butyl dicarbonate (3.04 g, 13.9 mmol) was added to a stirred solution of ((1r,4r)-4-aminocyclohexyl)methanol (1.50 g, 11.6 mmol) in tetrahydrofuran (20 mL). After stirring overnight at ambient temperature, the solvent was evaporated and the residue partitioned

DOI: 10.1021/acs.jmedchem.9b00533
J. Med. Chem. XXXX, XXX, XXX−XXX

Scheme 8. Pyridones: Early Introduction of Lipophilic Pocket Group[a]

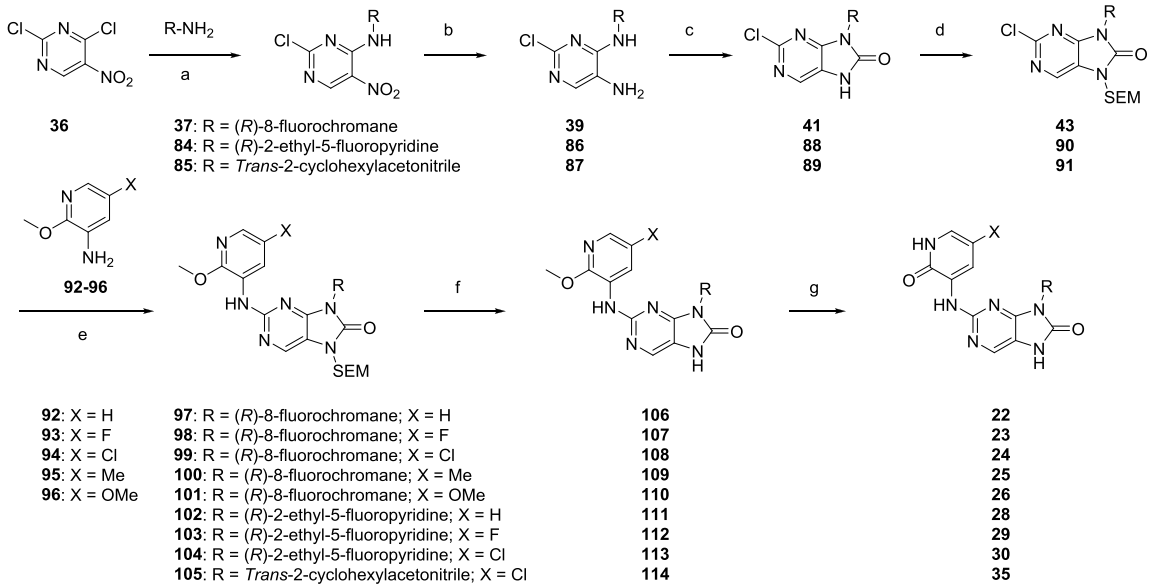

[a]Reagents and conditions: (a) R−NH_2, DIEA, CH_2Cl_2, −78 °C, 56−99%; (b) H_2, Pt/C, $ZnBr_2$, EtOAc, rt [R = (*R*)-8-fluorochromane, 75%]; H_2, Pd/C, EtOH, rt [R = (*R*)-2-ethyl-5-fluoropyridine, 30%] or $SnCl_2$, EtOH, reflux [R = *trans*-2-cyclohexylacetonitrile, 70%]; (c) CDI, CH_3CN, 80 °C, 63−99%; (d) NaH, SEM−Cl, DMF, 0 °C, 58−83%; (e) $Pd_2(dba)_3$, Xanthphos, Cs_2CO_3, dioxane, 110 °C, 33−81%; (f) TBAF, THF, 70 °C or trifluoroacetic acid, NH_3, MeOH, 60 °C, 56−97%; (g) TMSCl, NaI, CH_3CN, 80 °C, 45−96%.

Scheme 9. Synthesis of Aminopyridines 93−96[a]

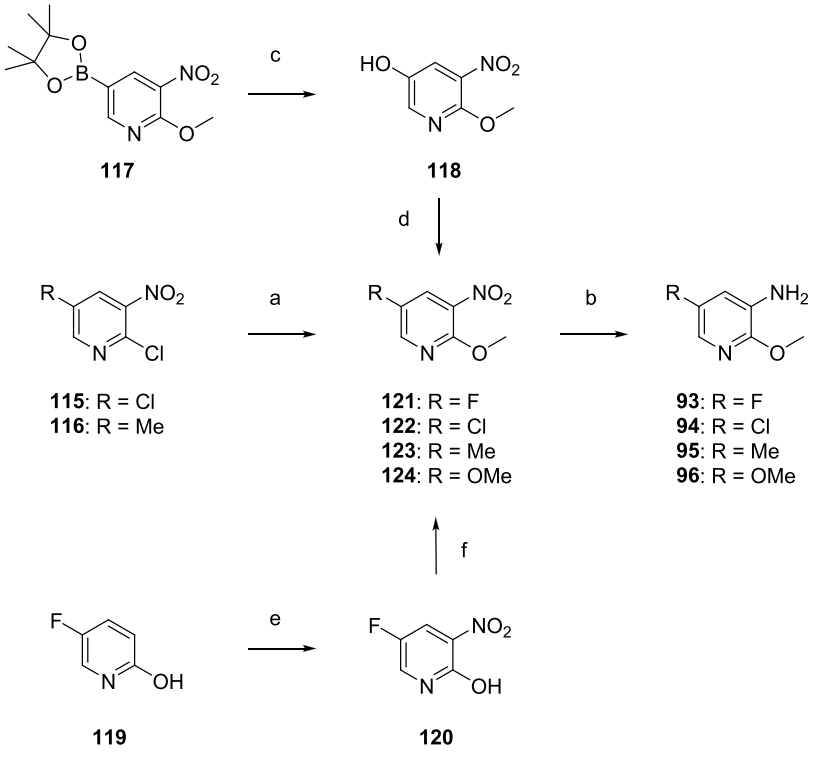

[a]Reagents and conditions: (a) NaOMe, MeOH, reflux, 78−87%; (b) H_2, Pd/C, EtOH, rt, 87−98% or H_2, Pt/C, $ZnBr_2$, EtOAc, rt (R = Cl, 99%); (c) H_2O_2, CH_2Cl_2, rt, 97%; (d) NaH, MeI, DMF, 0 °C to rt, 38%; (e) H_2SO_4, HNO_3, 0−85 °C, 43%; (f) MeI, Ag_2CO_3, $CHCl_3$, rt, 55%.

between ethyl acetate and water. The organic layer was separated, washed with water and brine, dried ($MgSO_4$), and the solvent was evaporated. The residue was treated with hexanes, and the suspension was filtered to give the title compound (2.11 g, 79%) as a white solid. Low-resolution mass spectrometry (LRMS) (*m*/*z*): 228 $(M - 1)^+$. ^1H NMR δ (300 MHz, DMSO-d_6): 0.84−0.95 (m, 2H), 1.05−1.18 (m, 2H), 1.20−1.29 (m, 2H), 1.40 (s, 9H), 1.71−1.80 (m, 3H), 3.14 (m, 1H), 3.21 (t, *J* = 5.8 Hz, 2H), 4.41 (t, *J* = 5.3 Hz, 1H), 6.73 (d, *J* = 8.2 Hz, 1H).

*((1r,4r)-4-(tert-Butoxycarbonylamino)cyclohexyl)methyl 4-Methylbenzene-sulfonate (**127**).* A solution of 4-methylbenzene-1-sulfonyl chloride (2.28 g, 11.96 mmol) in dichloromethane (10 mL) was

DOI: 10.1021/acs.jmedchem.9b00533
J. Med. Chem. XXXX, XXX, XXX−XXX

Scheme 10. Synthesis of Aminonitrile 129[a]

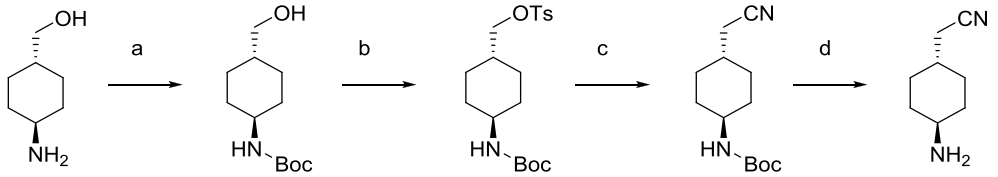

125 **126** **127** **128** **129**

[a]Reagents and conditions: (a) Boc_2O, THF, rt, 79%; (b) TsCl, CH_2Cl_2, Et_3N, rt, 83%; (c) NaCN, dimethyl sulfoxide (DMSO), 55 °C, 72%; (d) 4 N HCl, dioxane, rt, 89%.

Scheme 11. Pyridones: Early Introduction of the Hinge Binder Motif[a]

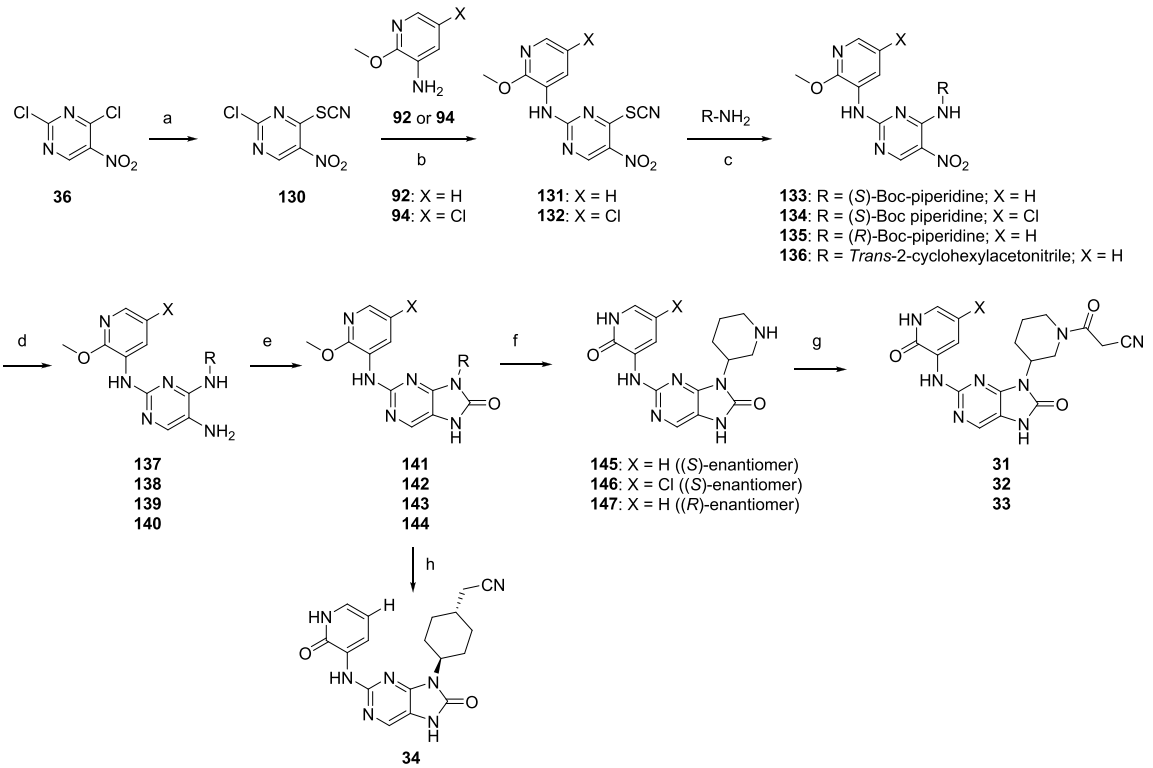

[a]Reagents and conditions: (a) KSCN, AcOH, 0 °C to rt, 63%; (b) **92**, Et_3N, EtOH, 0 °C (49%) or **94**, DIEA, THF, 0 °C (19%); (c) DIEA, THF, 50 °C, 21−99%; (d) H_2, Pd/C, EtOH, 88−99%; (e) CDI, CH_3CN, 70 °C, 21−85%; (f) 4 N HCl, dioxane, rt, 98−99%; (g) 2,5-dioxopyrrolidin-1-yl 2-cyanoacetamide, Et_3N, DMF, rt, 20−54%; (h) NaI, TMSCl, CH_3CN, 70 °C (81%).

added to a solution of *tert*-butyl (1r,4r)-4-(hydroxymethyl)-cyclohexylcarbamate **126** (2.11 g, 9.2 mmol) and triethylamine (1.59 mL, 11.4 mmol) in dichloromethane (50 mL), and the resulting mixture was stirred overnight at ambient temperature. The mixture was washed with 1 M aqueous sodium hydroxide solution, and the organic layer was dried ($MgSO_4$), evaporated, and the residue was purified by flash chromatography (diethyl ether/hexanes) to give the title compound (2.91 g, 83%) as a white solid. LRMS (*m*/*z*): 382 (M − 1)$^+$. ^{1}H NMR δ (300 MHz, $CDCl_3$): 0.90−1.12 (m, 4H), 1.43 (s, 3H), 1.87−1.68 (m, 2H), 2.10−1.90 (m, 2H), 3.34 (m, 1H), 3.48−3.41 (m, 1H), 3.81 (d, *J* = 6.5 Hz, 2H), 4.37 (m, 1H), 7.34 (d, *J* = 8.2 Hz, 2H), 7.77 (d, *J* = 8.2 Hz, 2H).

*tert-Butyl (1r,4r)-4-(Cyanomethyl)cyclohexylcarbamate (**128**).* Sodium cyanide (0.38 g, 7.8 mmol) was added to a solution of ((1r,4r)-4-(*tert*-butoxycarbonylamino)cyclohexyl)methyl 4-methylbenzene sulfonate **127** (1.00 g, 2.6 mmol) in dimethyl sulfoxide (10 mL), and the mixture was heated to 55 °C and stirred for 20 h. After cooling to room temperature, the reaction mixture was diluted with ethyl acetate; washed with saturated aqueous potassium carbonate solution, water, and brine; dried ($MgSO_4$); and the solvent was evaporated. The residue was purified by flash chromatography (100% dichloromethane to 95:5 dichloromethane/methanol) to give the title compound (0.450 g, 72%) as a white solid. LRMS (*m*/*z*): 239 (M + 1)$^+$. ^{1}H NMR δ (300 MHz, $CDCl_3$): 4.59−4.12 (m, 1H), 3.51−3.13 (m, 1H), 2.36−0.90 (m, 20H).

*2-((1r,4r)-4-Aminocyclohexyl)acetonitrile Hydrochloride (**129**).* A mixture of *tert*-butyl (1r,4r)-4-(cyanomethyl)cyclohexylcarbamate **128** (0.348 g, 1.46 mmol) and 4 M hydrogen chloride solution in dioxane (3.65 mL) was stirred overnight at ambient temperature. The solvent was evaporated in vacuo, and the residue was treated with diethyl ether. The resultant suspension was filtered to give the title compound (0.226 g, 89%) as a white solid. LRMS (*m*/*z*): 139 (M + 1)$^+$. ^{1}H NMR δ (300 MHz, DMSO-d_6): 8.08 (br s, 3H), 2.95 (d, *J* = 4.9 Hz, 1H), 2.50 (d, *J* = 6.5 Hz, 2H), 2.00 (d, *J* = 11.6 Hz, 2H), 1.83 (d, *J* = 12.3 Hz, 2H), 1.68−1.52 (m, 1H), 1.46−1.28 (m, 2H), 1.23−1.07 (m, 2H).

*2-Chloro-5-nitro-4-thiocyanatopyrimidine (**130**).* Potassium thiocyanate (2.10 g, 21.6 mmol) was added in portions over 2 h to a stirred solution of 2,4-dichloro-5-nitropyrimidine **36** (4.00 g, 20.6 mmol) in glacial acetic acid (25 mL) cooled to 10−15 °C using an

DOI: 10.1021/acs.jmedchem.9b00533
J. Med. Chem. XXXX, XXX, XXX−XXX

Scheme 12. Pyridones: Synthesis of Compound 27[a]

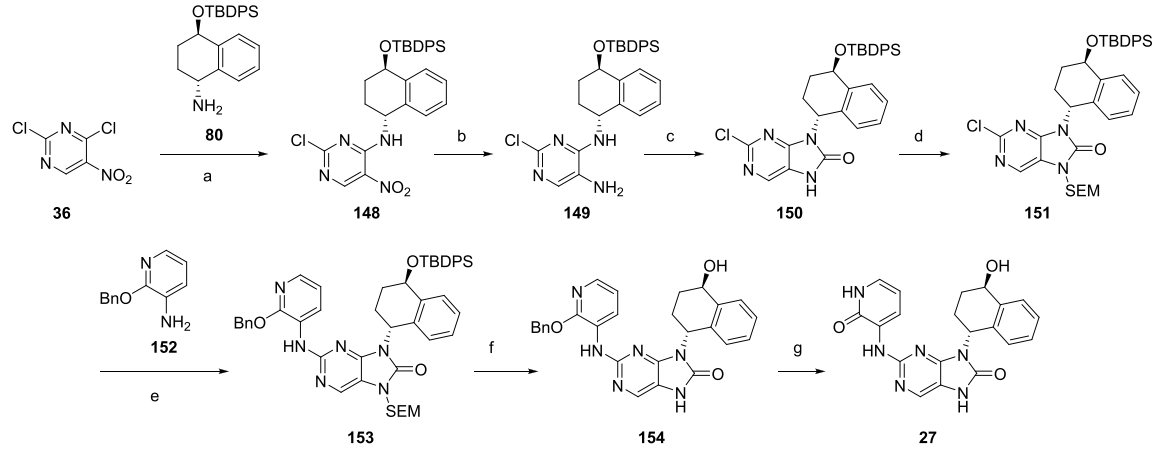

[a]Reagents and conditions: (a) DIEA, CH_2Cl_2, −78 °C, 95%; (b) $SnCl_2$, EtOH, 80 °C, 99%; (c) CDI, CH_3CN, 70 °C, 26%; (d) NaH, SEM−Cl, DMF, 0 °C, 71%; (e) $Pd_2(dba)_3$, Xanthphos, Cs_2CO_3, dioxane, 110 °C, 79%; (f) TBAF, THF, 70 °C, 45%; (g) H_2, Pd/C, THF/EtOAc, 88%.

ice−water bath. The mixture was then stirred at ambient temperature for 1 h, then diluted with water, and the precipitate was filtered, washed with water and ice-cold diethyl ether, and dried to give the title compound (2.82 g, 63%) as a white solid. ^{1}H NMR δ (300 MHz, $CDCl_3$): 9.40 (s, 1H).

*N-(2-Methoxypyridin-3-yl)-5-nitro-4-thiocyanatopyrimidin-2-amine (**131**).* 2-Methoxypyridin-3-amine **92** (0.100 g, 0.8 mmol) was added portionwise to a stirred, cooled (ice-bath) suspension of 2-chloro-5-nitro-4-thiocyanatopyrimidine **130** (0.174 g, 0.8 mmol) in ethanol (3 mL). Triethylamine (0.170 mL, 1.2 mmol) was then added dropwise, and the mixture was stirred for 30 min at 0 °C. The precipitate was filtered and dried to give the title compound (0.135 g, 49%) as a yellow solid. LRMS (m/z): 305 $(M + 1)^+$. ^{1}H NMR δ (300 MHz, DMSO-d_6): 3.95 (s, 3H), 7.03 (br s, 1H), 8.07 (br s, 1H), 9.24 (br s, 1H), 10.62 (s, 1H).

*2-((1r,4r)-4-(2-(2-Methoxypyridin-3-ylamino)-5-nitropyrimidin-4-ylamino)cyclohexyl)acetonitrile (**136**).* A mixture of *N*-(2-methoxypyridin-3-yl)-5-nitro-4-thiocyanatopyrimidin-2-amine **131** (0.178 g, 0.58 mmol), 2-((1r,4r)-4-aminocyclohexyl)acetonitrile hydrochloride **129** (0.123 g, 0.70 mmol), and *N*,*N*-diisopropylethylamine (0.62 mL, 3.5 mmol) in tetrahydrofuran (10 mL) was stirred and heated to 50 °C. After stirring overnight, the mixture was partitioned between water and ethyl acetate and the organic extract was washed with brine, dried ($MgSO_4$), and evaporated. The residue was purified by flash chromatography (0−50% ethyl acetate in hexanes) to give the title compound (0.109 g, 49%) as a white solid. LRMS (m/z): 384 $(M + 1)^+$. ^{1}H NMR δ (300 MHz, $CDCl_3$): 1.27−1.48 (m, 5H), 1.82 (m, 1H), 2.05 (d, J = 9.4 Hz, 2H), 2.28 (m, 2H), 2.41 (d, J = 6.0 Hz, 2H), 4.08 (s, 3H), 6.96 (dd, J = 7.7, 5.2 Hz, 1H), 7.90 (d, J = 4.9 Hz, 1H), 7.96 (m, 1H), 8.43 (m, 1H), 8.65 (d, J = 8.0 Hz, 1H), 9.08 (s, 1H).

*2-((1r,4r)-4-(5-Amino-2-(2-methoxypyridin-3-ylamino)pyrimidin-4-ylamino)cyclohexyl)acetonitrile (**140**).* 10% palladium on carbon (0.048 g) was added to a solution of 2-((1r,4r)-4-(2-(2-methoxypyridin-3-ylamino)-5-nitropyrimidin-4-ylamino)cyclohexyl)acetonitrile **136** (0.109 g, 0.28 mmol) in ethanol (15 mL), and the reaction mixture was stirred at ambient temperature under a hydrogen atmosphere. After 5 h, the mixture was then filtered through Celite and the filter cake was washed with ethanol. The combined filtrate and washings were concentrated to give the title compound (0.096 g, 96%) as an off-white solid. LRMS (m/z): 354 $(M + 1)^+$. ^{1}H NMR δ (300 MHz, $CDCl_3$): 1.19−1.43 (m, 4H), 1.76 (m, 1H), 2.06−1.95 (m, 2H), 2.30−2.17 (m, 2H), 2.35 (d, J = 6.5 Hz, 2H), 2.62 (s, 2H), 3.89−3.99 (m, 1H), 4.03 (s, 3H), 5.05 (d, J = 7.2 Hz, 1H), 6.87 (dd, J = 7.8, 5.0 Hz, 1H), 7.63 (s, 1H), 7.70 (dd, J = 5.0, 1.6 Hz, 1H), 8.69 (dd, J = 7.8, 1.6 Hz, 1H).

*2-((1r,4r)-4-(2-(2-Methoxypyridin-3-ylamino)-8-oxo-7H-purin-9(8H)-yl)cyclohexyl)acetonitrile (**144**).* A mixture of 2-((1r,4r)-4-(5-amino-2-(2-methoxypyridin-3-ylamino)pyrimidin-4-ylamino)-cyclohexyl)acetonitrile **140** (0.096 g, 0.27 mmol) and 1,1′-carbonylbis-1*H*-imidazole (0.088 g, 0.54 mmol) in acetonitrile (1.5 mL) was stirred and heated to 85 °C in a sealed tube. After 2 h, the solvent was evaporated and water was added to the residue. After stirring for 1 h at ambient temperature, the suspension was filtered and the solid was washed with water and dried to give the title compound (0.084 g, 74%) as an off-white solid. LRMS (m/z): 380 $(M + 1)^+$. ^{1}H NMR δ (300 MHz, DMSO-d_6): 1.23 (m, 6H), 1.83 (m, 2H), 2.04 (m, 2H), 2.42 (m, 1H), 4.01 (s, 3H), 4.08 (m, 1H), 7.05 (m, 1H), 7.83 (m, 1H), 7.88 (m, 1H), 8.03 (m, 1H), 8.58 (m, 1H), 11.13 (br s, 1H).

*2-((1r,4r)-4-(8-Oxo-2-(2-oxo-1,2-dihydropyridin-3-ylamino)-7H-purin-9(8H)-yl) cyclohexyl)acetonitrile (**34**).* Sodium iodide (2.43 g, 16.2 mmol) and trimethylsilyl chloride (2.05 mL, 16.2 mmol) were added to a suspension of 2-((1r,4r)-4-(2-(2-methoxypyridin-3-ylamino)-8-oxo-7*H*-purin-9(8*H*)-yl) cyclohexyl)acetonitrile **144** (2.05 g, 5.4 mmol) in acetonitrile (50 mL), and the mixture was stirred and heated to 85 °C in a sealed tube. After 2 h, the mixture was concentrated and treated with saturated aqueous sodium thiosulfate solution. After stirring for 30 min, the precipitate was filtered, washed with water and diethyl ether, and dried. The resulting solid was treated with hot ethanol, filtered, and dried to give the title compound (1.60 g, 81%) as a white solid. LRMS (m/z): 366 $(M + 1)^+$. HRMS calcd for $C_{18}H_{20}N_7O_2$: 366.16730. Found $[M + H]^+$: 366.16744. ^{1}H NMR δ (300 MHz, DMSO-d_6): 1.38−1.21 (m, 2H), 2.05−1.68 (m, 5H), 2.46−2.30 (m, 2H), 4.26−4.12 (m, 1H), 6.29−6.19 (m, 1H), 6.93 (d, J = 5.8 Hz, 1H), 8.01−7.89 (m, 2H), 8.29 (d, J = 7.1 Hz, 1H), 10.77 (br s, 1H), 11.61 (br s, 1H). ^{13}C NMR δ (151 MHz, DMSO-d_6): 23.4 (CH_2), 28.7 (CH_2), 31.1 (CH_2), 33.7 (CH), 51.2 (CH), 106.2 (CH), 116.1 (C), 117.7 (CH), 120.0 (C), 124.6 (CH), 130.9 (C), 133.8 (CH), 151.1 (C), 153.1 (C), 153.7 (C), 157.7 (C).

■ ASSOCIATED CONTENT

Supporting Information

The Supporting Information is available free of charge on the ACS Publications website at DOI: 10.1021/acs.jmedchem.9b00533.

Molecular formula strings (CSV)

General chemistry and biology experimental procedures (PDF)

Accession Codes

PDB codes are the following: 6HZV for **6**; 6HZU for **34**. The authors will release the atomic coordinates and experimental data upon article publication.

DOI: 10.1021/acs.jmedchem.9b00533
J. Med. Chem. XXXX, XXX, XXX−XXX

AUTHOR INFORMATION

Corresponding Author

*E-mail: jordi.bach@almirall.com.

ORCID

Jordi Bach: 0000-0002-0449-0161

Present Addresses

[#]Premiumlab S. L., Carretera Santa Creu de Calafell 49-B, Sant Boi de Llobregat, 08830 Barcelona, Spain (J.A.A.).

[▽]Research Center, Fundació ACE, Institut Català de Neurociències Aplicades, C/ Marquès de Sentmenat 57, 08029 Barcelona, Spain (A.O.).

[○]Admetra, C/General Ramon Despuig 17, 07013 Palma de Mallorca, Spain (J.A.).

[◆]Innoqua Toxicology Consultants, C/ Sant Antoni Maria Claret 272 2-2, 08041 Barcelona, Spain (A.A.).

[¶]IRB Barcelona-Institute for Research in Biomedicine, Parc Científic de Barcelona, C/Baldiri Reixac 10, 08028 Barcelona, Spain (N.P.).

[⋈]Peptinnovate, Stevenage Bioscience Catalyst, Gunnels Wood Road, Stevenage SG1 2FX, United Kingdom (J.D.A.).

[⧓]Montserrat Miralpeix Pharma Consulting, Parc Científic de Barcelona, C/ Baldiri Reixac 4-8, 08028 Barcelona, Spain (M.M.).

[⧖]Centro de Investigación Biomédica en Red de Diabetes y Enfermedades Metabólicas Asociadas (CIBERDEM), Hospital Duran i Reynals, Gran Via 199, 08908 L'Hospitalet de Llobregat, Barcelona, Spain (I.R.).

Author Contributions

The manuscript was written through contributions of all authors. All authors have given approval to the final version of the manuscript.

Funding

The authors were all full-time employees of Almirall S. A. at the time this work was completed and all funding for the work was provided by Almirall S. A.

Notes

The authors declare no competing financial interest.

ACKNOWLEDGMENTS

The authors thank Andreas Griessner, Alfred Lammens, Michael Blaesse, and Anja Jestel from Proteros Biostructures GmbH for X-ray structure determination of human JAK3 and JAK1 in complex with compounds **6** and **34** (PDB codes: 6HZV and 6HZU). They also acknowledge Eva Codesido, Raúl Fernández, Gloria Fra, María José Roó y Pablo Veiga from GalChimia S. A. for their contribution to the synthesis and scale-up of several of the compounds described in this article. They also thank Sonia Espinosa and Josep Maria Huerta for their support on physicochemical properties analysis and structural characterization of compounds, Mireia Verdú for her contribution to the evaluation of the activity of **34** in ion channels, and Elena Barceló for performing HRMS analysis of all tested compounds.

ABBREVIATIONS

ATP, adenosine triphosphate; AUC, area under the curve; BAL, bronchoalveolar lavage; Boc, *tert*-butyloxycarbonyl; CHO, Chinese hamster ovary; COPD, chronic obstructive pulmonary disease; GM-CSF, granulocyte-macrophage colony-stimulating factor; HPLC, high-performance liquid chromatography; HRMS, high-resolution mass spectrometry; IL, interleukin; JAK, Janus kinase; LPS, lipopolysaccharide; LRMS, low-resolution mass spectrometry; NMR, nuclear magnetic resonance; PAMPA, parallel artificial membrane permeability assay; PK, pharmacokinetics; PPB, plasma protein binding; SAR, structure−activity relationship; SEM, 2-(trimethylsilyl)ethoxymethyl; S_NAr, nucleophilic aromatic substitution; STAT, signal transducer and activator of transcription; TBAF, tetra-*n*-butylammonium fluoride; TBDPS, *tert*-butyldiphenylsilyl; Tyk2, tyrosine kinase 2; UPLC, ultraperformance liquid chromatography

REFERENCES

(1) Leonard, W. J.; O'Shea, J. J. JAKS and STATs: Biological implications. *Annu. Rev. Immunol.* **1998**, *16*, 293−322.

(2) Imada, K.; Leonard, W. J. The JAK-STAT pathway. *Mol. Immunol.* **2000**, *37*, 1−11.

(3) Yamaoka, K.; Saharinen, P.; Pesu, M.; Holt, V. E. T.; Silvennoinen, O.; O'Shea, J. J. The Janus kinases (Jaks). *Genome Biol.* **2004**, *5*, No. 253.

(4) O'Shea, J. J.; Pesu, M.; Borie, D. C.; Changelian, P. S. A new modality for immunosuppression: Targeting the JAK/STAT pathway. *Nat. Rev. Drug Discovery* **2004**, *3*, 555−564.

(5) Wilks, A. F. The JAK kinases: Not just another kinase drug discovery target. *Semin. Cell Dev. Biol.* **2008**, *19*, 319−328.

(6) Ghoreschi, K.; Laurence, A.; O'Shea, J. J. Janus kinases in immune cell signaling. *Immunol. Rev.* **2009**, *228*, 273−287.

(7) O'Shea, J. J.; Plenge, R. JAK and STAT signaling molecules in immunoregulation and immune-mediated disease. *Immunity* **2012**, *36*, 542−550.

(8) O'Shea, J. J.; Schwartz, D. M.; Villarino, A. V.; Gadina, M.; McInnes, I. B.; Laurence, A. The JAK-STAT pathway: Impact on human disease and therapeutic intervention. *Annu. Rev. Med.* **2015**, *66*, 311−328.

(9) Clark, J. D.; Flanagan, M. E.; Telliez, J.-B. Discovery and development of Janus kinase (JAK) inhibitors for inflammatory diseases. *J. Med. Chem.* **2014**, *57*, 5023−5038.

(10) Tam, C. S.; Verstovsek, S. Investigational Janus kinase inhibitors. *Expert Opin. Invest. Drugs* **2013**, *22*, 687−699.

(11) Taylor, V.; Siu, S.; Young, C.; Ste Marie, L.; Ren, H.; Leusink-Muis, T.; Van Ark, I.; Fokerts, G.; Park, G.; Pine, P.; Li, H.; Masuda, E. R256 is a potent and selective IL-13/4 receptor signaling inhibitor that reduces inflammation in a mouse model of chronic asthma. *Am. J. Respir. Crit. Care Med.* **2012**, *185*, No. A2843.

(12) Ashino, S.; Takeda, K.; Pine, P. R.; Gelfand, E. W. Janus kinase (JAK) 3 inhibitor, R256, attenuates allergen-induced airway hyperresponsiveness and airway inflammation in mice. *Am. J. Respir. Crit. Care Med.* **2012**, *185*, No. A2766.

(13) Jones, P.; Storer, R. I.; Sabnis, Y. A.; Wakenhut, F. M.; Whitlock, G. A.; England, K. S.; Mukaiyama, T.; Dehnhardt, C. M.; Coe, J. W.; Kortum, S. W.; Chrencik, J. E.; Brown, D. G.; Jones, R. M.; Murphy, J. R.; Yeoh, T.; Morgan, P.; Kilty, I. Design and synthesis of a pan-Janus kinase inhibitor clinical candidate (PF-06263276) suitable for inhaled and topical delivery for the treatment of inflammatory diseases of the lungs and skin. *J. Med. Chem.* **2017**, *60*, 767−786.

(14) Wiegman, C. H.; Russell, K. E.; Seiffert, J.; Rossios, C.; Adcock, I. M.; Rothaul, A.; Main, M.; Morgan, F. The selective pan-Janus kinase (JAK) inhibitor VR588 demonstrates potent anti-inflammatory activity in a murine chronic house dust mite (HDM) model of asthma. *Am. J. Respir. Crit. Care Med.* **2015**, *191*, No. A6435.

(15) Murray, P. J. The JAK-STAT signaling pathway: input and output integration. *J. Immunol.* **2007**, *178*, 2623−2629.

(16) Yew-Booth, L.; Birrell, M. A.; Lau, M. S.; Baker, K.; Jones, V.; Kilty, I.; Belvisi, M. G. JAK-STAT pathway activation in COPD. *Eur. Respir. J.* **2015**, *46*, 843−845.

(17) Vale, K. Targeting the JAK-STAT pathway in the treatment of 'Th2-high' severe asthma. *Future Med Chem.* **2016**, *8*, 405−419.

DOI: 10.1021/acs.jmedchem.9b00533
J. Med. Chem. XXXX, XXX, XXX−XXX

(18) Kudlacz, E.; Perry, B.; Sawyer, P.; Conklyn, M.; McCurdy, S.; Brissette, W.; Flanagan, A. M.; Changelian, P. The novel JAK-3 inhibitor CP-690550 is a potent immunosuppressive agent in various murine models. *Am. J. Transplant.* **2004**, *4*, 51−57.
(19) Ashino, S.; Takeda, K.; Li, H.; Taylor, V.; Joetham, A.; Pine, P. R.; Gelfand, E. W. Janus kinase 1/3 signaling pathways are key initiators of TH2 differentiation and lung allergic responses. *J. Allergy Clin. Immunol.* **2014**, *133*, 1162−1174.
(20) Ramis, I.; Calama, E.; Domènech, A.; Carreño, C.; Calaf, E.; Cordoba, M.; Albertí, J.; De Alba, J.; Bach, J.; Prats, N.; Miralpeix, M. New inhaled pan-JAK inhibitor A is efficacious at reducing allergen-induced airway inflammation in rat. *Am. J. Respir. Crit. Care Med.* **2014**, *189*, No. A4217.
(21) Calama, E.; Ramis, I.; Domènech, A.; Carreño, C.; De Alba, J.; Prats, N.; Miralpeix, M. Tofacitinib ameliorates inflammation in a rat model of airway neutrophilia induced by inhaled LPS. *Pulm. Pharmacol. Ther.* **2017**, 60−67.
(22) Ruwanpura, S. M.; McLeod, L.; Miller, A.; Jones, J.; Vlahos, R.; Ramm, G.; Longano, A.; Bardin, P. G.; Bozinovski, S.; Anderson, G. P.; Jenkins, B. J. Deregulated stat3 signaling dissociates pulmonary inflammation from emphysema in gp130 mutant mice. *Am. J. Physiol.: Lung Cell. Mol. Physiol.* **2012**, *302*, L627−L639.
(23) Mullings, R. E.; Wilson, S. J.; Puddicombe, S. M.; Lordan, J. L.; Bucchieri, F.; Djukanovic, R.; Howarth, P. H.; Harper, S.; Holgate, S. T.; Davies, D. E. Signal transducer and activator of transcription 6 (STAT-6) expression and function in asthmatic bronchial epithelium. *J. Allergy Clin. Immunol.* **2001**, *108*, 832−838.
(24) Christodoulopoulos, P.; Cameron, L.; Nakamura, Y.; Lemiere, C.; Muro, S.; Dugas, M.; Boulet, L. P.; Laviolette, M.; Olivenstein, R.; Hamid, Q. TH2 cytokine-associated transcription factors in atopic and nonatopic asthma: evidence for differential signal transducer and activator of transcription 6 expression. *J. Allergy Clin. Immunol.* **2001**, *107*, 586−591.
(25) Schwartz, D. M.; Kanno, Y.; Villarino, A.; Ward, M.; Gadina, M.; O'Shea, J. J. JAK inhibition as a therapeutic strategy for immune and inflammatory diseases. *Nat. Rev. Drug Discovery* **2017**, *16*, 843−862.
(26) Cooper, A. E.; Ferguson, D.; Grime, K. Optimisation of DMPK by the inhaled route: challenges and approaches. *Curr. Drug Metab.* **2012**, *13*, 457−473.
(27) Cole, A. G.; Bohnstedt, A. C.; Paradkar, V.; Kingsbury, C.; Quintero, J. G.; Park, H.; Lu, Y.; You, M.; Neagu, I.; Diller, D. J.; Letourneau, J. J.; Shao, Y.; James, R. A.; Riviello, C. M.; Ho, K. K.; Lin, T. H.; Wang, B.; Appell, K. C.; Sills, M.; Quadros, E.; Kimble, E. F.; Ohlmeyer, M. H.; Webb, M. L. 2-Benzimidazolyl-9-(chroman-4-yl)-purinone derivatives as JAK3 inhibitors. *Bioorg. Med. Chem. Lett.* **2009**, *19*, 6788−6792.
(28) Wu, G.; Robertson, D. H.; Brooks, C. L., III; Vieth, M. Detailed analysis of grid-based molecular docking: A case study of CDOCKER - A CHARMm-based MD docking algorithm. *J. Comput. Chem.* **2003**, *24*, 1549−1562.
(29) This series of purinone JAK inhibitors bearing an imidazo[1,2-*a*]pyridine hinge binder has been covered by the following patent application: Eastwood, P. R.; González, J.; Gómez, E.; Bach, J. Heteroaryl Imidazolone Derivatives as JAK Inhibitors. WO2011/157397, 2011.
(30) A similar approach using a pyrazolo[1,5-*a*]pyridine ring as hinge binder motif has been reported by Palau Pharmax: Almansa, C.; Salas, J.; Soliva, R.; Rodríguez, S.; Sicre, M. C. N-Containing Heteroaryl Derivatives as JAK3 Kinase Inhibitors. WO2011/051452, 2011.
(31) After the publication of Almirall's patent WO2011/157397, Ligand pharma also reported the use of an imidazo[1,2-a]pyridine ring as hinge binder motif for their JAK inhibitors: Cole, A. G.; James, R. A.; Shao, Y.; Letourneau, J. J.; Quintero, J. G.; Riviello, C. M.; Zhi, L. Janus Kinase Inhibitor and Methods. WO2013/025628, 2013.
(32) Chrencik, J. E.; Patny, A.; Leung, I. K.; Korniski, B.; Emmons, T. L.; Hall, T.; Weinberg, R. A.; Gormley, J. A.; Williams, J. M.; Day, J. E.; Hirsch, J. L.; Kiefer, J. R.; Leone, J. W.; Fischer, H. D.; Sommers, C. D.; Huang, H. C.; Jacobsen, E. J.; Tenbrink, R. E.; Tomasselli, A. G.; Benson, T. E. Structural and thermodynamic characterization of the TYK2 and JAK3 kinase domains in complex with CP-690550 and CMP-6. *J. Mol. Biol.* **2010**, *400*, 413−433.
(33) Williams, N. K.; Bamert, R. S.; Patel, O.; Wang, C.; Walden, P. M.; Wilks, A. F.; Fantino, E.; Rossjohn, J.; Lucet, I. S. Dissecting specificity in the Janus kinases: the structures of JAK-specific inhibitors complexed to the JAK1 and JAK2 protein tyrosine kinase domains. *J. Mol. Biol.* **2009**, *387*, 219−232.
(34) This screening selectivity panel was mainly formed by kinases inhibited by JAK inhibitors (29) and completed with a selection of diverse representative kinases from the whole kinome (7). Kinases inhibited by JAK inhibitors have been identified through literature analysis and internal profiling of competitors' compounds. List of selected kinases from the kinome includes EGFR, IGF-1R, IKKα, JNK1α1, JNK2α2, MEK1 and TAK1. JAK inhibitors described in this article have shown poor activity when tested against kinases not included in this panel.
(35) Compound **34** was negative for genotoxicity with and without metabolic activation in the GreenScreen HC assays performed at Gentronix (highest concentration tested: 39 μg/mL). In the Ames II, Ames MPF and Ames MPF *E. coli* Combo mutagenicity assay performed at Xenometrix, **34** proved to be negative in all strains at the concentrations tested (highest concentration tested: 1581 μg/mL).

DOI: 10.1021/acs.jmedchem.9b00533
J. Med. Chem. XXXX, XXX, XXX−XXX